computation

Article

Spatial Diversity for CDMA RoFSO Links over M Turbulence Channels with Nonzero Boresight Pointing Errors

Michalis P. Ninos and Hector E. Nistazakis *

Department of Electronics, Computers, Telecommunications and Control, Faculty of Physics, National and Kapodistrian University of Athens, Athens 15784, Greece; ninmichail@phys.uoa.gr
* Correspondence: enistaz@phys.uoa.gr; Tel.: +30-210-727-6710

Received: 9 September 2018; Accepted: 25 October 2018; Published: 28 October 2018

Abstract: A CDMA RoFSO link with receivers' spatial diversity is studied. Turbulence-induced fading, modeled by the M(alaga) distribution, is considered that hamper the FSO link performance along with the nonzero boresight pointing errors effect. Novel, analytical closed-form expressions are extracted for the estimation of the average bit-error-rate and the outage probability of the CDMA RoFSO system for both directions of the forward and the reverse link. The numerical results show clearly the performance improvement of using spatial diversity, even in the most adverse atmospheric conditions with strong and saturated atmospheric turbulence with enhanced misalignment. Also, the effects of nonlinear distortion, multiple access interference and clipping noise aggravate the performance of the link, where cases with large number of users are taken into account.

Keywords: free-space optical communications; spatial diversity; RoFSO; CDMA; malaga distribution; nonzero boresight pointing errors

1. Introduction

Free-space optical (FSO) systems have emerged over the last few years as a valuable solution for broadband networks, providing performance features with high data rate applications and high security transmission due the narrow optical beam [1]. Analogue intensity modulation (AIM) technique comprises a low cost and simple modulation technique for optical communications, which finds applications in cable TV (CATV) distributions, radio-over-fiber (RoF), radio-on-free-space optics (RoFSO) etc. [2]. RoFSO systems constitute a relatively new wireless technology with the similar aim to the RoF technique of distributing radio frequency (RF) signals among central base stations (CBS) and remote antenna units (RAU) (Figure 1) [3,4].

However, FSO links experience the detrimental influence of atmospheric-related phenomena such as atmospheric turbulence, pointing errors (PE), beam wander, atmospheric attenuation etc., [5–13]. Turbulence-induced irradiance fluctuations are studied statistically and many statistical distribution models have been proposed over the years, according the specific turbulence conditions. In the weak turbulence regime the log-normal and the gamma distribution models have been proven that describe accurately the statistics of the irradiance fluctuations. From weak up to strong turbulence conditions the gamma-gamma model constitutes a very accurate model while for strong and saturate turbulence conditions the K and the negative exponential models are the most suitable [5]. Recently, the M(alaga) model has been proposed in the literature, which has the significant advantage of unifying almost all the previous-mentioned distribution models as special cases [6]. Additionally, PE impairments are also considered a serious degradation factor for FSO systems [7,8]. In this work, we employ a new generalized PE model that approximates the Beckmann distribution with a modified Rayleigh distribution. In this model, nonzero boresight (NZB) displacement and different spatial jitters for the axes of the receiver are taken into account [9].

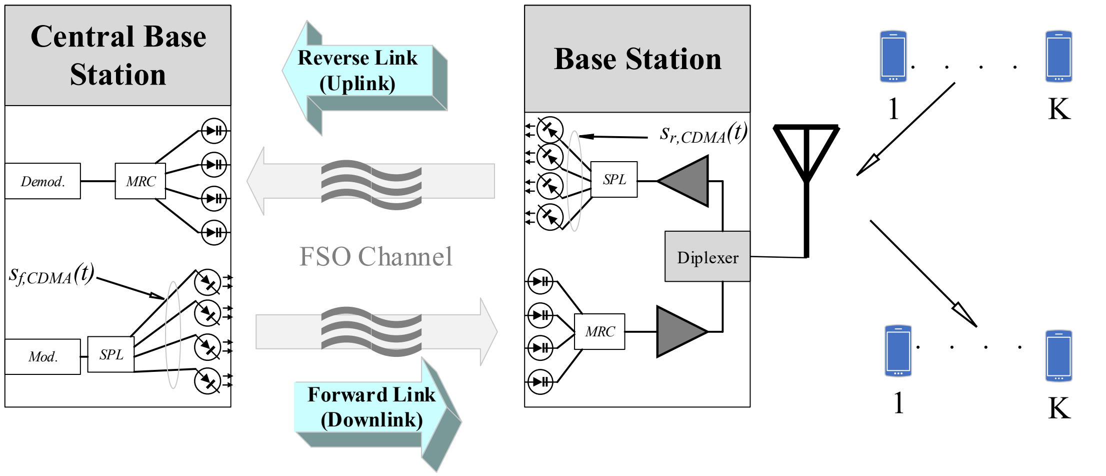

Figure 1. The system model for the CDMA RoFSO system with spatial diversity for both directions of the forward and the reverse link. (SPL: splitter, MRC: maximum ratio combiner).

In order to mitigate the influence of the atmospheric turbulence and the PE, diversity schemes have been proposed and used [1,2,14–17]. Spatial diversity technique can be realized when a multitude of transmit or receive apertures are employed [1,2]. In the present work, we assume a RoFSO system with spatial diversity on the receivers and multiple laser sources at the transmitter. Each one of the laser sources is directed towards a specific receiver. The objective of this configuration is to harness the maximum optical radiation for each diversity branch.

Code-division multiple access (CDMA) is a widely used multiple access technique, where multiple users communicate using the same band of frequency. CDMA is based on the spread spectrum (SS) technique where each user is provided with a unique spreading code. CDMA was commercially adopted in the cellular standards of IS-95, IS-2000 and UMTS, [18]. It is also considered, for potential applications in the future cellular standards, in combination with orthogonal frequency division multiple access (OFDMA), [4].

Thus, in this work we investigate a RoFSO system with receivers' spatial diversity for transmission of CDMA signals. The specific CDMA RoFSO system is studied in both, the forward and the reverse link. The performance evaluation is carried out with the average bit error rate (ABER) and the outage probability (OP) estimation, taking into account nonlinear effects related to the optical link, the multiple access interference (MAI), the atmospheric turbulence effect modeled by the M-distribution and the NZB PE. Closed-form expressions are extracted for the aforementioned performance metrics and numerical results are illustrated using the derived expressions.

2. The CDMA RoFSO System with Spatial Diversity

2.1. Forward Link

A thorough analysis of the CDMA point to point (P2P) RoFSO link is presented in Ref. [19]. The proposed spatially diverse system is composed of M-individual P2P links, where a set of M laser emitters transmit towards an array of M receivers. So, at the CBS K CDMA user's signals proceed for optical transmission through the wireless spatially diverse optical link. Each laser transmitter is linked with a specific receiver as it can be seen in Figure 1. In the case of the forward link transmission, the detected carrier to noise plus interference power ratio for each k-th user ($CNIR_k$) in a specific m-th P2P link is given as, [19]:

$$CNIR_{k,f,m}(I_m) \approx \frac{(m_{k,m}\rho_m L_{tot,m} P_0 I_m)^2}{2\left(\langle N_{0,m}B\rangle_{AV} + \left\langle n_{NLD,f,k,m}\right\rangle_{AV}\right)}, \tag{1}$$

where the subscript symbol f denotes the forward link, $m_{k,m}$ is the optical modulation index (OMI) for each user, ρ_m is the optoelectronic conversion ratio of the photo-detector (PD), $L_{tot,m}$ corresponds to the total losses of the P2P wireless optical link due to path loss, geometrical loss etc., P_0 is the average transmitted optical power and I_m is the total normalized instantaneous irradiance at the receiver's input. The random variable of I_m is a product of two random factors which correspond to the atmospheric turbulence $I_{t,m}$ and the PE $I_{p,m}$ i.e., $I_m = I_{t,m}I_{p,m}$. The power spectral density $N_{0,m}$ of the optical link noise for the mth receiver is given as, [4,19]:

$$N_{0,m} = N_{th,m} + N_{shot,m} + N_{RIN,m} = \frac{4K_BT}{R_L} + 2qI_{ph,m} + {I_{ph,m}}^2(RIN)\left(1 + \sum_{k=1}^{K} m_{k,m}^2\left\langle s_k^2(t)\right\rangle\right), \tag{2}$$

where K_B is the Boltzmann's constant, T is the absolute temperature, R_L is the receiver circuit load resistor, q is the electron charge, RIN is the relative intensity noise factor of the laser diode (LD) and $I_{ph,m}$ is the dc value of the photo-induced current at the mth receiver and is given as $I_{ph,m} = \rho_m L_{tot,m} P_0 I_m = \rho_m P_{R,m} I_m$ with $P_{R,m}$ being the average received optical power at the mth receiver. The parameter B is the bandpass filter bandwidth of the receiver centered at the RF carrier frequency f_c. We assume that the receivers have very narrow field of view (FOV) and employ optical bandpass filters (OBPF) in the form of coatings on the receivers' optics. The OBPF have $\Delta\lambda < 1$ nm in order to reduce significantly the background radiation I_B from the sun and the sky. In case this is not happened, the background noise contributes to the shot noise term i.e., $N_{shot,m} = 2q\left(I_{ph,m} + I_{B,m}\right)$, [2] (Equation (2.44)). Finally, the total nonlinear distortion for the forward link, i.e., $n_{NLD,f,m}$, is a sum of the 3rd order inter-modulation distortion (IMD3) and the clipping distortion $n_{NLD,f,k,m} = \sigma^2_{IMD,f,k,m} + \sigma^2_{cl,k,m}$ which are given as, [19]:

$$\sigma^2_{IMD,f,k,m} = \frac{9\alpha_3^2 m_{k,m}^6 (K-1) I_{ph,m}^2}{128} \tag{3}$$

and

$$\sigma^2_{cl,k,m} = \frac{I_{ph,m}^2 m_{k,m}^6 K^3}{27.2}\exp\left(-\frac{1}{2m_{k,m}^2 K}\right) \tag{4}$$

2.2. Reverse Link

On the reverse link, K CDMA user's signals arrive at the antenna base station at a specific time instant and the carrier to noise plus interference power ratio for each kth user ($CNIR_k$) in a P2P link is given as [19]:

$$CNIR_{k,r,m}(I) \approx \frac{(m_{k,m}\rho_m L_{tot,m} P_0 I_m)^2}{2(\langle N_{0,m}B\rangle_{AV} + \langle n_{NLD,r,k,m}\rangle_{AV})}, \tag{5}$$

where the subscript symbol r denotes the reverse link and all the parameters are the same as the aforementioned for the forward link except for the total nonlinear distortion on the reverse link, i.e., $n_{NLD,r,k,m}$. The $n_{NLD,rk,m}$ is a sum of the 3rd order inter-modulation distortion (IMD3) of the reverse link, the clipping distortion given in (4) and the generated MAI due to the asynchronous transmission $n_{NLD,r,k,m} = \sigma^2_{IMD,r,k,m} + \sigma^2_{cl,k,m} + \sigma^2_{MAI,k,m}$. The IMD3 for the case of the reverse link and the MAI are evaluated as [19]:

$$\sigma^2_{IMD,r,k,m} = \frac{\left(m_{k,m}I_{ph,m}\right)^2}{2}\left[\frac{\alpha_3 m_{k,m}^2(2K-1)(K-1)}{8G_p} + \frac{\alpha_3^2 m_{k,m}^4(K-1)}{64}\left(9 + \frac{252K^2 + 300K - 648}{10G_p}\right)\right] \tag{6}$$

and

$$\sigma^2_{MAI,k,m} = \left(m_{k,m} I_{ph,m}\right)^2 \frac{K-1}{12G_p} \tag{7}$$

In his analysis Pursley demonstrated that the amount of the MAI for an asynchronous spread spectrum system from $K-1$ other active users is quantified as $MAI \approx (K-1)/3G_p$ [18] (Equation (3.63)). Therefore, the process gain G_p is tha main parameter for the pseudo-random (PN) code sequences that is taken into account. A perception of the system model for both directions of the forward and the reverse link is illustrated in Figure 1.

2.3. Spatial Diversity Receivers

A spatial diversity scheme is employed on the receivers' side, along with a maximum ratio combining (*MRC*) scheme. Multiple copies of the same radio frequency (RF) CDMA signal are transmitted from an array of M optical laser sources towards a set of M photo-detector apertures at the receiver. The spacing between the laser sources at the transmitter and the receive apertures at the receiver is larger than the spatial coherence length of the atmospheric channel, i.e., a few centimeters, in order to achieve uncorrelated and independent diversity branches. Thus, the signals from each diversity branch are weighted with a gain factor G_m, which is proportional to the signal strength in the specific diversity branch. They are co-phased and summed coherently. The output of the *MRC* combiner is given as [2,20]:

$$CNIR_{k,MRC}(I) = \sum_{m=1}^{M} CNIR_{k,m}(I_m) = r(t), \tag{8}$$

The output of the *MRC* combiner is sent to a K-dimension matched filter receiver, where the desired signal of the 1st user, denoted as $y_1(n)$, is given in [18] (Equation (6.40)). The specific process can be implemented in both directions of the forward and the reverse link. The details of the spatial diversity is shown in Figure 2.

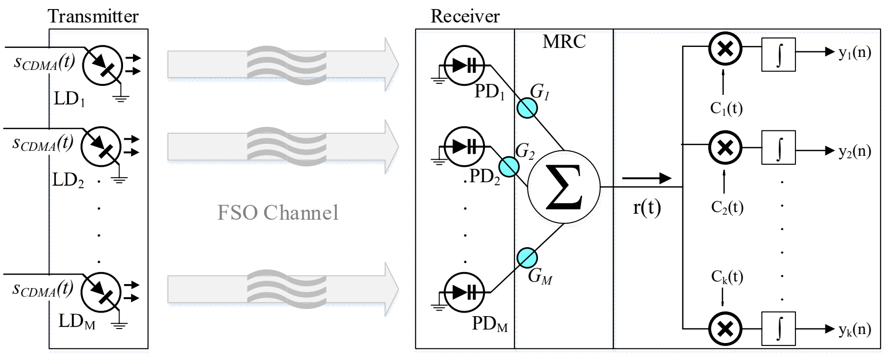

Figure 2. Block diagram of the CDMA RoFSO system with receivers' spatial diversity.

3. The *M*-Distribution with Nonzero Boresight Pointing Errors

In this section, the M distributed turbulence model with NZB PE is investigated. In [8], the probability density function (PDF) of the combined effects for a P2P link has been extracted as:

$$\begin{aligned} f_{comb,I_m}(I_m) = \frac{\xi^2_{\text{mod},m} A^{(\aleph\ or\ \Re)}}{2} I_m^{-1} \sum_{j=1}^{(\aleph\ or\ \Re)} a_j^{(\aleph\ or\ \Re)} \left(B^{(\aleph\ or\ \Re)}\right)^{-\frac{\alpha_m+j}{2}} \times \\ \times G_{1,3}^{3,0}\left(B^{(\aleph\ or\ \Re)} \frac{I_m}{A_{\text{mod},m}} \middle| \begin{array}{c} \xi^2_{\text{mod},m}+1 \\ \xi^2_{\text{mod},m},\ \alpha_m,\ \beta_m \end{array} \right) \end{aligned} \tag{9}$$

where $G_{p,q}^{m,n}[\cdot]$ stands for the Meijer G-function [21] (Equation (9.301)). The M-distribution is divided in two categories, which are determined by the value of the β_m parameter [6]. In this work, we take into account only the case of β_m being a natural number, i.e., $\beta_m \in \aleph$. In this case, the summation in (6) takes the form $\sum_{(\aleph)}[.] = \sum_{j=1}^{\beta}[.]$ and the parameters $A^{(\aleph)}$, $a_j^{(\aleph)}$ and $B^{(\aleph)}$ are given as $A^{(\aleph)} = \left(2\alpha_m^{\alpha_m/2}(\gamma_m\beta_m)^{\beta_m+\frac{\alpha_m}{2}}\right) / \left(\gamma_m^{(2+\alpha_m)/2}\Gamma(\alpha_m)(\gamma_m\beta_m+\Omega'_m)^{\beta_m+\frac{\alpha_m}{2}}\right)$ $a_j^{(\aleph)} = \begin{pmatrix} \beta_m - 1 \\ j-1 \end{pmatrix} \frac{1}{(j-1)!}\left(\frac{\Omega'_m}{\gamma_m}\right)^{j-1}\left(\frac{\alpha_m}{\beta_m}\right)^{j/2}(\gamma_m\beta_m+\Omega'_m)^{1-\frac{j}{2}}$, $B^{(\aleph)} = \frac{\alpha_m\beta_m}{\gamma_m\beta_m+\Omega'_m}$ where $\begin{pmatrix} \beta_m \\ j \end{pmatrix}$ represents the binomial coefficient, [6,8].

The parameter $\xi_{mod,m}$ related to the NZB PE effect is calculated as $\xi_{\text{mod},m} = W_{z,eq,m}/2\sigma_{\text{mod},m}$ with $\sigma_{mod,m}$ being, [9]:

$$\sigma_{\text{mod},m} = \left(\frac{3\mu_{x,m}^2\sigma_{x,m}^4 + 3\mu_{y,m}^2\sigma_{y,m}^4 + \sigma_{x,m}^6 + \sigma_{y,m}^6}{2}\right)^{1/6}, \tag{10}$$

where $\mu_{x,m}$, $\mu_{y,m}$, $\sigma_{x,m}$ and $\sigma_{y,m}$ are parameters of the Beckmann PDF and correspond to the spatial jitters on the horizontal and the elevation axis ($\sigma_{x,m}$, $\sigma_{y,m}$) of each receiver and the fixed boresight displacements ($\mu_{x,m}$, $\mu_{y,m}$) of the optical beam center from the center of the mth receiver for the two vertical axis. The other parameter $A_{mod,m}$, is given as, [9]:

$$A_{\text{mod},m} = A_{0,m}\exp\left(\frac{1}{\xi_{\text{mod},m}^2} - \frac{1}{2\xi_{x,m}^2} - \frac{1}{2\xi_{y,m}^2} - \frac{\mu_{x,m}^2}{2\sigma_{x,m}^2\xi_{x,m}^2} - \frac{\mu_{y,m}^2}{2\sigma_{y,m}^2\xi_{y,m}^2}\right) \tag{11}$$

where $\xi_{x,m} = W_{z,eq,m}/2\sigma_{x,m}$ and $\xi_{y,m} = W_{z,eq,m}/2\sigma_{y,m}$ with $W_{z,eq,m}$ being the equivalent beam radius at the receiver and is given through the expression $W_{z,eq,m}^2 = \sqrt{\pi}erf(v_m)W_{z,m}^2/2v_m\exp(-v_m^2)$. The parameter $A_{0,m}$ is the fraction of the collected power at $r = 0$ and equals to $A_{0,m} = [erf(v_m)]^2$ with $v_m = \sqrt{\pi}R_m/\sqrt{2}W_{z,m}$, where $erf(.)$ represents the error function and $W_{z,m}$ is the footprint of the Gaussian beam on each receiver plane [7–10,13]. The parameter $W_{z,m}$ under strong fluctuation conditions equals $W_{z,m} = W_{0,m}\sqrt{\Theta_{0,m}^2 + \Lambda_{0,m}^2}\sqrt{1+1.63\sigma_R^{12/5}\Lambda_m}$ with $\sigma_R^2 = 1.23C_n^2k^{7/6}L_{S,m}^{11/6}$ being the Rytov variance and $\Lambda_m = \frac{\Lambda_{0,m}}{\Theta_{0,m}^2+\Lambda_{0,m}^2}$, $\Theta_{0,m} = 1 - \frac{L_{S,m}}{F_{0,m}}$, $\Lambda_{0,m} = \frac{2L_{S,m}}{kW_{0,m}^2}$, $k = 2\pi/\lambda$, [5]. The parameter $W_{0,m}$ is the beam spot radius at each transmitter, $L_{S,m}$ is the link distance for each diversity link and $F_{0,m}$ is the phase front radius of curvature. In our case we assume a convergent beam with $F_{0,m} > 0$. Finally, the 1st order moment, i.e., the expected value, of the total normalized irradiance I_m is calculated as $E[I_m] = \int_0^{\infty} I_m f_{comb,I_m}(I_m)dI_m$ and its closed-form expression, for $\beta_m \in \aleph$, is given as [10]:

$$E[I_m]^{\aleph} = \frac{\xi_{\text{mod},m}^2 A_{\text{mod},m}}{\xi_{\text{mod},m}^2 + 1}(\gamma_m + \Omega'_m) \tag{12}$$

4. Average Bit Error Rate Estimation

In this section, mathematical expressions are extracted for the estimation of the ABER metric of the kth user for the proposed spatially diverse link. In the specific CDMA RoFSO link with receivers' diversity, each user's signal is modulated with an *L-QAM* modulation. Gray code mapping is used at the transmitter and the conditional BER for the *L-QAM* constellation with the *MRC* output signal is given as, [22]:

$$P_{b,k,QAM,MRC}(I_m) = \frac{4\left(1 - L^{-1/2}\right)}{\log_2(L)}Q\left(\sqrt{\frac{3}{L-1}\sum_{m=1}^{M} CNIR_{k,m}(I_m)}\right). \tag{13}$$

The ABER for each user, $P_{b,k,MRC,AV}$, of the CDMA RoFSO link with diversity reception technique over M turbulence channels and NZB PE, is estimated by solving the following multiple integrals, [14,15]:

$$P_{b,k,AV} = \int_{\vec{I}} f_{comb,\vec{I}}\left(\vec{I}\right) P_{b,k,QAM,MRC}\left(\vec{I}\right) d\vec{I} \tag{14}$$

where the vector $\vec{I} = (I_1, I_2, \ldots, I_M)$ consists of all the irradiance values for each link of the receivers diversity scheme [17].

Thus, taking into account the following approximation for the Q-function [23]:

$$Q(x) \approx \frac{1}{12}\left[\exp\left(-\frac{x^2}{2}\right) + 2\exp\left(-2x^2\right) + 2\exp\left(-\frac{2x^2}{3}\right)\right] \tag{15}$$

and by using the Equation (13), we conclude to the following integrals:

$$\begin{aligned} P_{b,k,AV} \approx \tfrac{1-L^{-1/2}}{3\log_2(L)} \Bigg[& \int_0^\infty f_{comb,I_m}(I_m) \exp\left(\frac{3\sum_{m=1}^{M} CNIR_{k,m}(I_m)}{2(1-L)}\right) dI_m + \\ & +2\int_0^\infty f_{comb,I_m}(I_m) \exp\left(\frac{6\sum_{m=1}^{M} CNIR_{k,m}(I_m)}{1-L}\right) dI_m + 2\int_0^\infty f_{comb,I_m}(I_m) \exp\left(\frac{2\sum_{m=1}^{M} CNIR_{k,m}(I_m)}{1-L}\right) dI_m \Bigg] \end{aligned} \tag{16}$$

The irradiance values, I_m, are statistically independent and identically distributed (i.i.d.) random variables. Due to the independency of the I_m vectors, the M-fold integral in (16) is partitioned into a product of M one-dimensional integrals, [24]. As a result, we obtain the following expression for the estimation of the ABER:

$$\begin{aligned} P_{b,k,AV} \approx \tfrac{1-L^{-1/2}}{3\log_2(L)} \Bigg[& \prod_{m=1}^{M} \int_0^\infty f_{comb,I_m}(I_m) \exp\left(-\tfrac{3CNIR_{k,m}(I_m)}{2(L-1)}\right) dI_m + \\ & +2\prod_{m=1}^{M} \int_0^\infty f_{comb,I_m}(I_m) \exp\left(-\tfrac{6CNIR_{k,m}(I_m)}{L-1}\right) dI_m + \\ & +2\prod_{m=1}^{M} \int_0^\infty f_{comb,I_m}(I_m) \exp\left(-\tfrac{2CNIR_{k,m}(I_m)}{L-1}\right) dI_m \Bigg] \end{aligned} \tag{17}$$

Next, we replace the exponential terms with the equivalent Meijer-G expressions for the exponential function, i.e., $\exp(z) = G_{0,1}^{1,0}(-z|0)$, and we get:

$$\begin{aligned} P_{b,k,AV} \approx \tfrac{1-L^{-1/2}}{3\log_2(L)} \Bigg[& \prod_{m=1}^{M} \int_0^\infty f_{comb,I_m}(I_m) G_{0,1}^{1,0}\left(\tfrac{3CNIR_{k,m}(I_m)}{2(L-1)} \middle| \, 0\right) dI_m + \\ & +2\prod_{m=1}^{M} \int_0^\infty f_{comb,I_m}(I_m) G_{0,1}^{1,0}\left(\tfrac{6CNIR_{k,m}(I_m)}{L-1} \middle| \, 0\right) dI_m + \\ & +2\prod_{m=1}^{M} \int_0^\infty f_{comb,I_m}(I_m) G_{0,1}^{1,0}\left(\tfrac{2CNIR_{k,m}(I_m)}{L-1} \middle| \, 0\right) dI_m \Bigg] \end{aligned} \tag{18}$$

Substituting for the $f_{comb,I_m}(I_m)$ from (9) and using the formula from [25] (Equation (21)), we conclude to the following closed-form expression for the estimation of the ABER of each user on the CDMA RoFSO link with receivers' diversity and L-QAM modulation:

$$P_{b,k,AV} \approx \frac{1-L^{-1/2}}{3\log_2(L)}\left(\prod_{m=1}^{M}\Psi\left(\frac{3}{2},m\right) + 2\prod_{m=1}^{M}\Psi(6,m) + 2\prod_{m=1}^{M}\Psi(2,m)\right) \tag{19}$$

with $\Psi(x,m) = \frac{\xi^2_{\text{mod},m} A^{(\aleph)}}{2} \sum_{j=1}^{\beta} a_j^{(\aleph)} \left(B^{(\aleph)}\right)^{-\frac{\alpha_m+j}{2}} \frac{2^{\alpha_m+j-2}}{2\pi} \Xi_j(x,m)$ and $\Xi_j(x,m) = G^{1,6}_{6,3}\left(\frac{16xCNIR_{k,m,EX} A^2_{\text{mod},m}}{(L-1)\left(B^{(\aleph)} E[I]^{(\aleph)}\right)^2} \middle| \begin{matrix} \frac{1-\xi^2_{\text{mod},m}}{2}, \frac{2-\xi^2_{\text{mod},m}}{2}, \frac{1-\alpha_m}{2}, \frac{2-\alpha_m}{2}, \frac{1-j}{2}, \frac{2-j}{2} \\ 0, -\frac{\xi^2_{\text{mod},m}}{2}, \frac{1-\xi^2_{\text{mod},m}}{2} \end{matrix} \right)$.

5. Outage Probability Estimation

The OP for a P2P CDMA RoFSO link has been derived in [19] as:

$$P_{out,m,k} = \frac{\xi^2_{\text{mod},m} A^{(\aleph)}}{2} \sum_{j=1}^{\beta} a_j^{(\aleph)} \left(B^{(\aleph)}\right)^{-\frac{\alpha_m+j}{2}} \times \\ \times G^{3,1}_{2,4}\left(\frac{B^{(\aleph)} E[I_m]^{(\aleph)}}{A_{\text{mod},m}} \sqrt{\frac{CNIR_{k,m,th}}{CNIR_{k,m,EX}}} \middle| \begin{matrix} 1,\ \xi^2_{\text{mod},m}+1 \\ \xi^2_{\text{mod},m},\ \alpha_m,\ \beta_m,\ 0 \end{matrix} \right) \tag{20}$$

Thus, the OP for the spatially diverse link with M statistically independent links is given as [16] (Equation (10)):

$$P_{out,k} = \prod_{m=1}^{M} P_{out,m,k}. \tag{21}$$

6. Numerical Results

In this section, appropriate numerical results are illustrated, using the derived closed-form expressions (19) and (21). Several parameter values are chosen for the CDMA RoFSO link with receivers' spatial diversity. Firstly, we assume two different cases for the atmospheric turbulence conditions. In the first case we assume strong irradiance fluctuations with the value of the Rytov variance equal to $\sigma_R^2 = 2.5$ and in the second case we choose saturate turbulence conditions with $\sigma_R^2 = 25$. The aperture radius for each receiver is chosen equal to $R_m = 5$ cm. The beam spot radius at each transmitter is $W_{0,m} = 3$ cm, the operational wavelength $\lambda = 1.55$ μm, the link distance $L_{S,m} =$ 1.5 km and the phase front radius is $F_{0,m} = 500$ m. The beam spot radius at each receiver aperture is calculated equal to $W_{z,m} = 9$ cm for $\sigma_R^2 = 2.5$ and $W_{z,m} = 25$ cm for $\sigma_R^2 = 25$. For the CDMA RoFSO link we have the IMD3 coefficient equal to $\alpha_3 = 1/3$, $G_p = 512$, $T = 300$ K and $RIN = -155$ dB/Hz. The load resistance is $R_L = 50\ \Omega$ and $<s_k(t)> = 1$. Also, the bandwidth for the forward link is chosen $B = 20$ MHz while for the reverse link is $B = 10$ MHz. For the influence of the PE effect, two cases are considered. For the first case, we select weak spatial jitters with normalized values at $\sigma_x/R = 0.2$ and $\sigma_y/R = 0.1$ and zero boresight displacement i.e., $\mu_x/R = 0$ and $\mu_y/R = 0$. In the second case, enhanced spatial jitters are considered, with $\sigma_x/R = 0.5$, $\sigma_y/R = 0.2$ and NZB displacement with $\mu_x/R = 0.1$ and $\mu_y/R = 0.1$.

The selected modulation scheme for the forward link is the 16-QAM, while for the reverse link is the QPSK. The ABER results for the CDMA RoFSO link with receivers' diversity are illustrated among the Figures 3–6 wherein cases with $M = 2 \times 2$ and $M = 4 \times 4$ transceivers are shown. In Figures 2 and 3 the ABER performance of the forward link is presented. In Figure 3 the weak PE case is depicted and in Figure 4 the strong PE impact is shown. It is deduced that an average received optical power per diversity branch ($P_{R,m}$) above -10 dBm is required for the case of the forward link when $M = 4$ transceivers are used in order to attain an ABER at 10^{-4} even in the saturated turbulence conditions, i.e., $\sigma_R^2 = 25$. In the case of enhanced PE impact, i.e., Figure 3, the performance slightly worsens and the required $P_{R,m}$ increases proportionally.

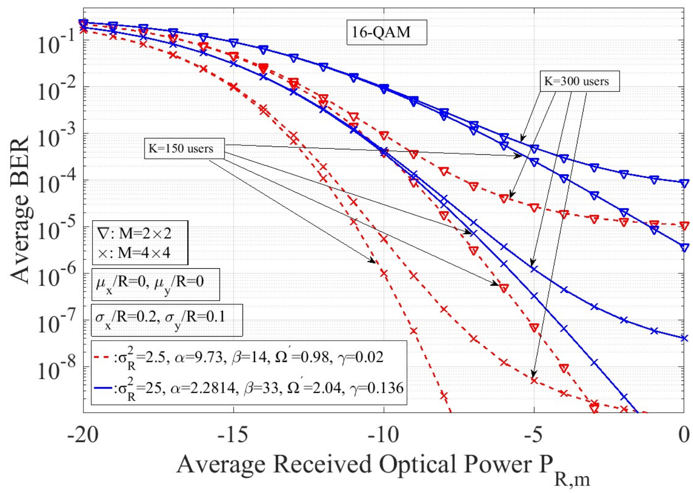

Figure 3. The ABER performance for the forward CDMA RoFSO link with receivers' diversity, over strong turbulence and weak PE impact for different values of the number of users *K*.

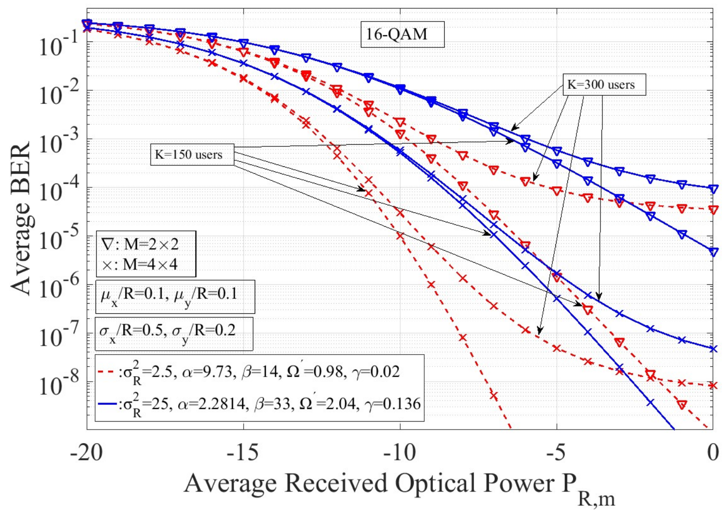

Figure 4. The ABER performance for the forward CDMA RoFSO link with receivers' diversity, over strong turbulence and enhanced PE impact for different values of the number of users *K*.

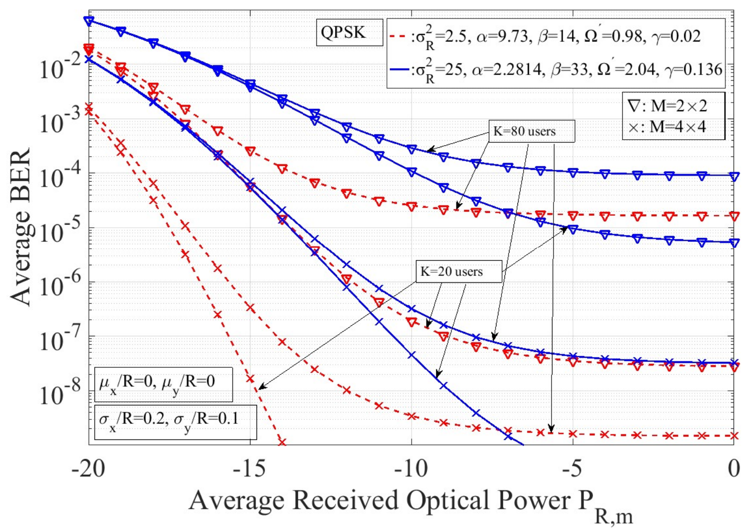

Figure 5. The ABER performance for the reverse CDMA RoFSO link with receivers' diversity, over strong turbulence and weak PE impact for different values of the number of users *K*.

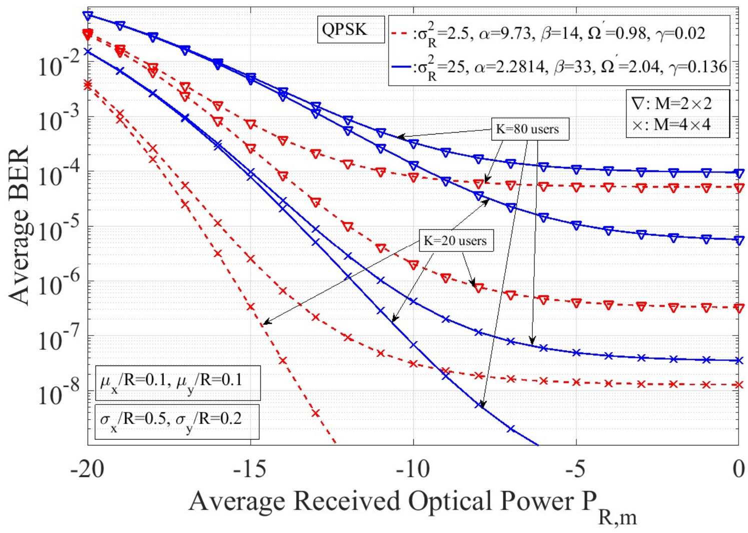

Figure 6. The ABER performance for the reverse CDMA RoFSO link with receivers' diversity, over strong turbulence and enhanced PE impact for different values of the number of users *K*.

The ABER performance for the reverse link of the CDMA RoFSO system is illustrated in Figures 5 and 6. Firstly, as it is illustrated in both figures the simultaneous access of 80 users is feasible, especially when $M = 4$ transceivers are employed. In this case, the required $P_{R,m}$ is -15 dBm for ABER at 10^{-4} with saturated turbulence conditions. The case of enhanced PE is presented in Figure 4, where the performance exacerbates primarily in the case of $\sigma_R^2 = 2.5$.

Eventually, the OP outcomes are depicted in Figures 7 and 8. It is worth noting that the outage performance estimation is implemented as a function of the $CNIR_{k,m,EX}$, providing the advantage for performance assessment of both directions of the forward and the reverse link. Compared to the case of the P2P link, [18], the OP touches significantly lower values and the availability of the link increases. The threshold value for the $CNIR_{k,th}$ per diversity branch is fix equal to 10 dB. In the case of $M = 4 \times 4$, the spatially diverse link performs very well even at saturated turbulence conditions with values of the $CNIR_{k,EX}$ per branch at 20 dB for both directions of the forward and the reverse link.

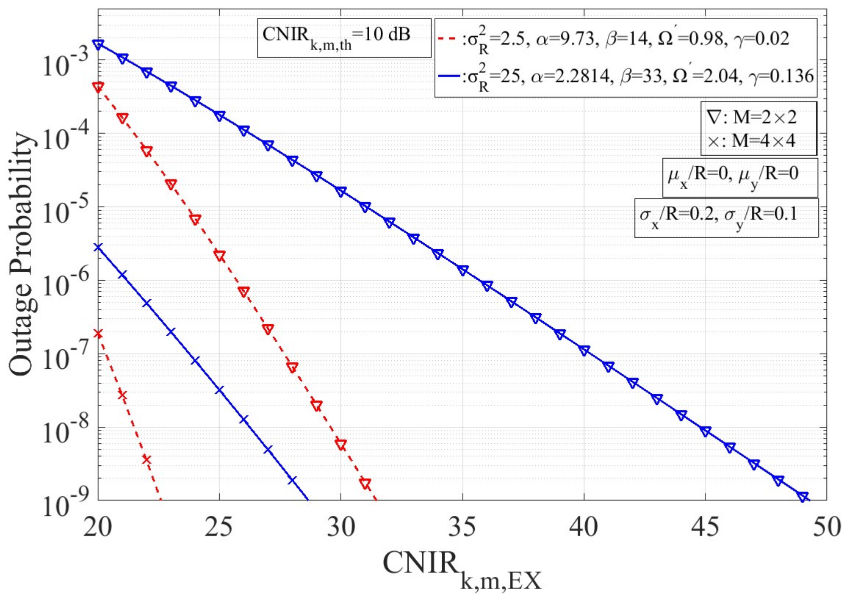

Figure 7. The OP for the CDMA RoFSO link with receivers' diversity for both directions, over strong turbulence and weak PE impact as a function of the $CNIR_{k,EX}$ per branch.

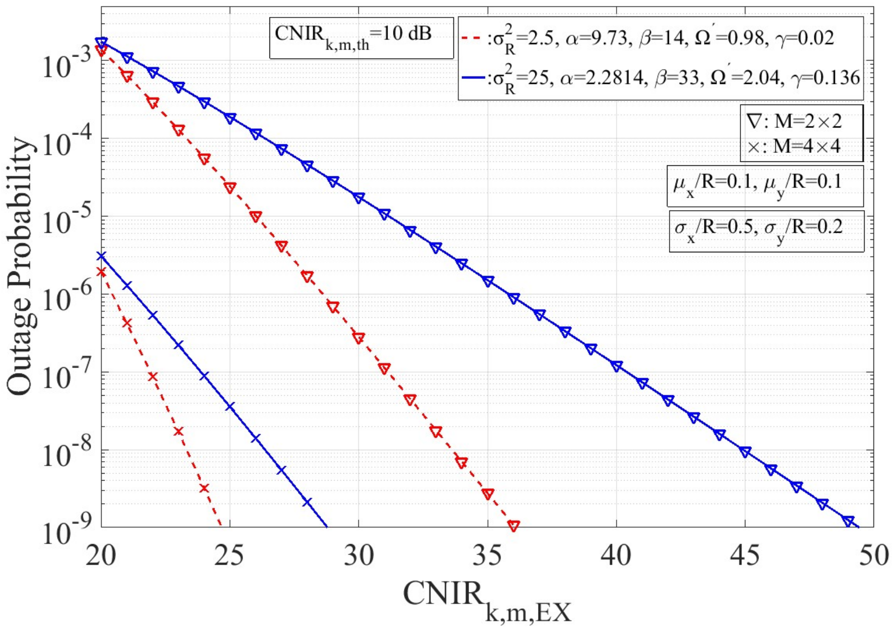

Figure 8. The OP for the CDMA RoFSO link with receivers' diversity for both directions, over strong turbulence and strong PE impact as a function of the $CNIR_{k,EX}$ per branch.

7. Conclusions

In this work, a RoFSO link for CDMA signal transmission with receivers' diversity is studied. An array of *M* laser sources transmits towards an array of *M* receivers. Analytical closed-form mathematical expressions are obtained for the estimation of the ABER and the OP, which are used for the numerical performance estimation of the specific system for both, the forward and the reverse link. As it is presented, the CDMA RoFSO link operates adequately well with the spatial diversity scheme even in the worst case scenarios of saturated atmospheric turbulence conditions with enhanced PE influence. Also, in the derived numerical simulations a large number of users are considered that simultaneously access the network for the cases of the forward and the reverse link. The latter situation implies that the effects of IMD, MAI and clipping distortion are also immense.

Author Contributions: M.P.N. carried out the mathematical analysis and simulation results of the manuscript. H.E.N. confirmed their validity.

Funding: This research received no external funding.

Conflicts of Interest: The authors declare no conflict of interest.

References

1. Uysal, M.; Capsoni, C.; Ghassemlooy, Z.; Boucouvalas, A.; Udvary, E. (Eds.) *Optical Wireless Communications: An Emerging Technology*; Springer: Cham, Switzerland, 2016; ISBN 978-3-319-30201-0.
2. Ghassemlooy, Z.; Popoola, W.; Rajbhandari, S. *Optical Wireless Communications: System and Channel Modelling with Matlab*; CRC Press, Taylor & Francis Group: Boca Raton, FL, USA, 2012; ISBN 9781138074804.
3. Kazaura, K.; Wakamori, K.; Matsumoto, M.; Higashino, T.; Tsukamoto, K.; Komaki, S. RoFSO: A universal platform for convergence of fiber and free space optical communication networks. *IEEE Commun. Mag.* **2010**, *48*, 130–137. [CrossRef]
4. Fernando, X.N. *Radio over Fiber for Wireless Communications: From Fundamentals to Advanced Topics*; Wiley: Hoboken, NJ, USA, 2014; ISBN 978-3-319-30201-0.
5. Andrews, L.C.; Philips, R.L. *Laser Beam Propagation through Random Media*; SPIE: Bellingham, WA, USA, 2005; ISBN 9780819459480.

6. Jurado-Navas, A.; Garrido-Balsells, J.M.; Paris, J.F.; Puerta-Notario, A. A unifying statistical model for atmospheric optical scintillation. In *Numerical Simulation in Physics and Engineering*; Intech Publisher: Rijeka, Croatia, 2011; pp. 181–206.
7. Farid, A.; Hranilovic, S. Outage capacity optimization for free-space optical links with pointing errors. *J. Lightw. Technol.* **2007**, *25*, 1702–1710. [CrossRef]
8. Jurado-Navas, A.; Garrido-Balsells, J.M.; Paris, J.F.; Castillo-Vasquez, M.; Puerta-Notario, A. Impact of pointing errors on the performance of generalized atmospheric optical channels. *Opt. Express* **2012**, *20*, 12550–12562. [CrossRef] [PubMed]
9. Boluda Ruiz, R.; Garcia-Zambrana, A.; Castillo-Vazquez, C.; Castillo-Vázquez, B. Novel approximation of misalignment fading modeled by Beckmann distribution on free-space optical links. *Opt. Express* **2016**, *24*, 22635–22649. [CrossRef] [PubMed]
10. Ansari, I.S.; Yilmaz, F.; Alouini, M.S. Performance Analysis of Free-Space Optical Links over Málaga (M) Turbulence Channels with Pointing Errors. *IEEE Trans. Wirel. Commun.* **2016**, *15*, 91–102. [CrossRef]
11. Varotsos, G.K.; Nistazakis, H.E.; Petkovic, M.I.; Djordjevic, G.T.; Tombras, G.S. SIMO optical wireless links with nonzero boresight pointing errors over *M* modeled turbulence channels. *Opt. Commun.* **2017**, *403*, 391–400. [CrossRef]
12. Muhammad, S.S.; Kohldolfer, P.; Leitgeb, E. Channel Modeling for Terrestrial Free Space Optical Links. In Proceedings of the 7th International Conference of Transparent Optical Networks, Barcelona, Spain, 3–7 July 2005.
13. Ales, P. Atmospheric effects on availability of free space optics systems. *Opt. Eng.* **2009**, *48*, 066001. [CrossRef]
14. Navidpour, S.M.; Uysal, M.; Kavehrad, M. BER performance of free space optical transmission with spatial diversity. *IEEE Trans. Wirel. Commun.* **2007**, *6*, 2813–2819. [CrossRef]
15. Tsiftsis, T.A.; Sandalidis, H.G.; Karagiannidis, G.K.; Uysal, M. Optical wireless links with spatial diversity over strong atmospheric turbulence channels. *IEEE Trans. Wirel. Commun.* **2009**, *8*, 951–957. [CrossRef]
16. Zixiong, W.; Wen-De, Z.; Songnian, F.; Chinlon, L. Performance comparison of different modulation formats over free-space optical (FSO) turbulence links with space diversity reception technique. *IEEE Photonics J.* **2009**, *1*, 277–285. [CrossRef]
17. Nistazakis, H.E. A time-diversity scheme for wireless optical links over exponentially modeled turbulence channels. *Optik* **2013**, *124*, 1386–1391. [CrossRef]
18. Abu-Rgheff, M.A. *Introduction to CDMA Wireless Communications*; Academic Press: New York, NY, USA, 2007; ISBN 978-0-7506-5252-0.
19. Ninos, M.P.; Nistazakis, H.E.; Sandalidis, H.G.; Tombras, G.S. CDMA RoFSO links with nonzero boresight pointing errors over *M* turbulence channels. *IEEE Photonics J.* **2018**, 10. [CrossRef]
20. Simon, M.K.; Alouini, M.S. *Digital Communications over Fading Channels*, 2nd ed.; Wiley-IEEE: Hoboken, NJ, USA, 2004; pp. 401–415, ISBN 978-0-471-64953-3.
21. Gradshteyn, I.S.; Ryzhik, I.M. *Table of Integrals, Series, and Products*, 7th ed.; Academic Press: New York, NY, USA, 2007; ISBN 978-0-7506-5252-0.
22. Proakis, J.G.; Salehi, M. *Digital Communications*, 5th ed.; McGraw-Hill: New York, NY, USA, 2008; ISBN 978-0072957167.
23. Sadhwani, D.; Yadav, R.N.; Aggrawal, S. Tighter bounds on the Gaussian Q function and its application in Nakagami-m fading channel. *IEEE Wirel. Commun. Lett.* **2017**, *6*, 574–577. [CrossRef]
24. Alouini, M.S.; Simon, M.K. An MGF-based performance analysis of generalized selection combining over Rayleigh fading channels. *IEEE Trans. Commun.* **2000**, *48*, 401–415. [CrossRef]
25. Adamchik, V.S.; Marichev, O.I. The Algorithm for calculating integrals of hypergeometric type function and its realization in reduce system. In Proceedings of the International Symposium on Symbolic and Algebraic Computation, Tokyo, Japan, 20–24 August 1990; pp. 212–214. [CrossRef]